Video Article

Decellularization of Whole Human Heart Inside a Pressurized Pouch in an Inverted Orientation

Doris A. Taylor[1], Luiz C. Sampaio[1], Rafael Cabello[1], Abdelmotagaly Elgalad[1], Rohan Parikh[1], R Patrick Wood[2], Kevin A. Myer[2], Alvin T. Yeh[3], Po-Feng Lee[1]

[1]Regenerative Medicine Research, Texas Heart Institute

[2]Lifegift Organ Donation Center

[3]Biomedical Engineering, Texas A&M University

Correspondence to: Doris A. Taylor at DTaylor@texasheart.org

URL: https://www.jove.com/video/58123
DOI: doi:10.3791/58123

Keywords: Bioengineering, Issue 141, Pressure head, pericardium, decellularization, turbidity, human heart, flow dynamics

Date Published: 11/26/2018

Citation: Taylor, D.A., Sampaio, L.C., Cabello, R., Elgalad, A., Parikh, R., Wood, R.P., Myer, K.A., Yeh, A.T., Lee, P.F. Decellularization of Whole Human Heart Inside a Pressurized Pouch in an Inverted Orientation. *J. Vis. Exp.* (141), e58123, doi:10.3791/58123 (2018).

Abstract

The ultimate solution for patients with end-stage heart failure is organ transplant. But donor hearts are limited, immunosuppression is required, and ultimately rejection can occur. Creating a functional, autologous bio-artificial heart could solve these challenges. Biofabrication of a heart comprised of scaffold and cells is one option. A natural scaffold with tissue-specific composition as well as micro- and macro-architecture can be obtained by decellularizing hearts from humans or large animals such as pigs. Decellularization involves washing out cellular debris while preserving 3D extracellular matrix and vasculature and allowing "cellularization" at a later timepoint. Capitalizing on our novel finding that perfusion decellularization of complex organs is possible, we developed a more "physiological" method to decellularize non-transplantable human hearts by placing them inside a pressurized pouch, in an inverted orientation, under controlled pressure. The purpose of using a pressurized pouch is to create pressure gradients across the aortic valve to keep it closed and improve myocardial perfusion. Simultaneous assessment of flow dynamics and cellular debris removal during decellularization allowed us to monitor both fluid inflow and debris outflow, thereby generating a scaffold that can be used either for simple cardiac repair (*e.g.* as a patch or valve scaffold) or as a whole-organ scaffold.

Video Link

The video component of this article can be found at https://www.jove.com/video/58123/

Introduction

Heart failure leads to high mortality in patients. The ultimate treatment option for end-stage heart failure is allo-transplantation. However, there is a long wait-list for transplantation due to the shortage of donor organs, and patients face post-transplantation hurdles that range from life-long immunosuppression to chronic organ rejection[1,2]. Bioengineering functional hearts by repopulating decellularized human-sized hearts with a patient's own cells could circumvent these hurdles[3].

A major step in "engineering" a heart is the creation of a scaffold with appropriate vascular and parenchymal structure, composition and function to guide the alignment and organization of delivered cells. In the presence of the appropriate framework, cells seeded on the scaffold should recognize the environment and perform the expected function as part of that organ. In our opinion, decellularized organ extracellular matrix (dECM) comprises the necessary characteristics of the ideal scaffold.

By utilizing intrinsic vasculature, complex whole-organ decellularization can be achieved via antegrade or retrograde perfusion[4] to remove cellular components while preserving the delicate 3D extracellular matrix and vasculature[2,5,6,7]. A functional vasculature is important in bioengineering whole organs just as it is *in vivo*, for nutrient distribution and waste removal[8]. Coronary perfusion decellularization has been proven to be effective in creating decellularized hearts from rats[4], or pigs[4,7,9,10,11,12,13], and humans[5,7,14,15,16]. Yet, integrity of the valves, atria and other "thin" regions can suffer.

Human-size decellularized heart scaffolds can be obtained from pigs using pressure control[7,9,10,11,12] or infusion flow rate control[13,17] and from human donors using pressure control[5,7,14,15]. Decellularization of human donor hearts occurs over 4-8 days under pressure controlled at 80-100 mmHg in upright orientation[5,15,16] or over 16 days under pressure controlled at 60 mmHg[14]. Under antegrade, pressure-controlled decellularization, the aortic valve competency plays a crucial role in maintaining coronary perfusion efficiency and stable pressure at the aortic root. Our previous work revealed that the orientation of the heart influences its coronary perfusion efficiency during the decellularization procedure and therefore the scaffold integrity in the end[9].

As a continuation of our previous work[9], we introduce a novel concept wherein a pericardium-like pouch is added to improve whole-heart decellularization. We describe the decellularization of human hearts placed inside pressurized pouches, inversely oriented, and under pressure controlled at 120 mmHg at the aortic root. This protocol includes monitoring the flow profile and collection of outflow media throughout the

decellularization procedure to evaluate coronary perfusion efficiency and cell debris removal. Biochemical assays are then performed to test the effectiveness of the method.

Protocol

All experiments adhered to the ethics committee guidelines from the Texas Heart Institute.

1. Organ Preparation

NOTE: In collaboration with LifeGift, a nonprofit organ procurement organization in Texas (http://www.lifegift.org), donated human hearts not suitable for transplant were used for research with approved consent.

1. To procure hearts, intravenously infuse 30,000 U heparin to the hearts. Securely suture cardioplegia cannula in the aorta and attach a clamped perfusion line. Perforate the inferior vena cava (IVC) to vent the right heart. Cut either the left superior pulmonary vein or the left atrial appendage to vent the left chambers of the heart.
2. Infuse 1 L of cardioplegia or heparinized saline. Dissect aortic arch branches, superior vena cava (SVC) and other pulmonary veins to release the heart from any vascular or surrounding tissue attachment. Submerge the well-heparinized heart in iced saline solution.
3. Inspect the donated human heart (both anteriorly and posteriorly, **Figure 1**). Place the heart on a dissecting tray and inspect for any structural damage or anatomical malformations. If liver and/or lungs were procured for transplantation, the heart may present with a short inferior vena cava and/or absence of left atrial posterior wall.
4. Perform internal inspection for possible defects - atrial septal defect (ASD), ventricular septal defect (VSD), or valve (aortic, pulmonary, mitral, tricuspid) malformation.
5. If a septal defect is present, correct it with appropriate sutures (**Figure 2A, 2B**). The correction of septal defects is needed to monitor decellularization progress via pulmonary artery (PA) outflow turbidity measurement. Correction of the septal defect removes left to right shunt, hence, the outflow from PA represents the outflow from the coronary circulation through the coronary sinus.
6. Ligate superior and inferior vena cava with 2-0 silk suture (**Figure 2C**).
7. Dissect the aorta (Ao) away from the main PA (**Figure 2D**) for subsequent cannulation.
8. Insert connectors, based on the diameter of the vessel, (**Figure 3**) into Ao and PA and secure them with 2-0 silk sutures (**Figure 4A**).
9. Insert a tubing line through the left atrium (**Figure 4B**) and toward the left ventricle (LV) (**Figure 3**), using one of the pulmonary vein orifices.
10. Connect an infusion line to the connector placed in the Ao and the outflow line to the one in the PA (**Figure 3**).
11. Place the prepared heart into a polyester pouch in inverted orientation (upside down).
12. Place the pouch with heart into a perfusion container and close the lid (**Figure 4C**).
13. Connect each of the lines to the respective ports in the rubber stopper (based on the diameter of container) and insert it to the lid of the perfusion container to seal the polyester pouch (**Figure 4C** and **Figure 5B**).
14. Perfuse 1x phosphate buffered saline (PBS) (136 mM NaCl, 2.7 mM KCl, 10 mM Na_2HPO_4 and 1.8 mM KH_2PO_4 in distilled water, pH 7.4) via the infusion port of the rubber stopper to verify outflow from the PA and from the line inserted into LV.
15. Use this flow to clean the organ of any residual traces of blood in the vasculature. If flow is not observed, tighten the connection lines as they might be loose.

2. System Setup and Organ Decellularization Procedure

1. Assemble the bioreactor and place in an upright orientation (**Figure 5**). The perfusion system includes a personal computer (PC), proportional-integral-derivative (PID) controller, a peristaltic pump for Ao infusion, a perfusion bioreactor, a pressure head container for LV perfusate retention (2L aspirator bottle with bottom sidearm), and a peristaltic pump to drain excess fluid from the pressure head container and to collect the outflow from PA.
2. In the rubber septum, connect the infusion line, pressure-head line, PA-outflow line and bioreactor draining line to the rubber cap surface ports placed on top of the perfusion bioreactor (**Figure 5A**).
3. Decellularize hearts under constant pressure of 120 mmHg measured at the aortic root. Mean pressure of the LV should be within 14-18 mmHg throughout the whole decellularization process.
4. Decellularize hearts as follows: 4 h of hypertonic solution (500 mM NaCl), 2 h of hypotonic solution (20 mM NaCl), 120 h of sodium dodecyl sulfate (1% SDS) solution, and a final wash with 120 L of 1X PBS (**Figure 6A**).
5. Decellularize the hearts under constant pressure control (120 mmHg). Infusion flow rate into Ao is heart-dependent and is, on average, 98.06±16.22 mL/min for hypertonic solution, 76.14±7.90 mL/min for hypotonic solution, 151.50±5.76 mL/min for SDS, and 185.24±7.10 mL/min for PBS. The total consumed volume of each reagent averages 23.36±5.70 L for hypertonic solution and 9.13±1.26 L for hypotonic solution.
6. Recirculate the final 60 L of 1% SDS (1 L per gram of heart weight) until the end of SDS perfusion. **Figure 6A** shows a timeline for the decellularization process, eliciting endpoints for data collection: flow rate monitoring (Ao and PA) and outflow collection (PA and non-PA) from pressure head during decellularization.
7. Since the SVC and IVC are ligated, it is reasonable to assume that all fluid collected from the PA is the result of actual coronary perfusion (**Figure 5B**). Determine coronary perfusion efficiency by directly dividing the flow rate of perfusate out of the PA by the flow rate of infused solution into Ao:

   Coronary perfusion efficiency = $\frac{flow\ rate\ out\ of\ PA}{flow\ rate\ into\ Ao}$ (%).
8. Perform comparative analysis of the perfusate obtained from the PA and the LV and the infused solutions in duplicate by loading 200 µL per well in a clear bottom 96-well plate and reading absorbance at 280 nm. The absorbance value, selected empirically after trying different values, was found to give the best normalized values.

9. Use the turbidity of clean infused reagent as the control. The turbidity of the outflow perfusate represents washout of cell debris and can be quantified instantly during decellularization as a tracking tool of the process.
10. During the final wash with 10 L of 1X PBS, add 500 mL of sterile neutralized 2.1% peracetic acid solution, neutralized with 10N NaOH, leading to a 0.1% peracetic acid solution (v/v) in PBS. Use this solution to sterilize the scaffold.

3. Evaluation of Decellularized Hearts

NOTE: After decellularization, representative hearts will be used for coronary angiogram imaging and biochemical assays.

1. Perform coronary angiography of the representative decellularized human heart to examine the intactness of the coronary vasculature. Briefly, using a fluoroscope, image decellularized human heart after injection of contrast agent through coronary ostial cannula in the main right and left coronary arteries.
2. Dissect the decellularized heart to get samples from 19 areas to evaluate the remaining deoxyribonucleic acid (DNA), glycosaminoglycan (GAG) and SDS levels in decellularized tissues. Remove the base of the heart from ventricles and dissect the ventricles into 4 equal sections (**Figure 6C**). Divide each section into the anterior and posterior right ventricle (RV), the anterior and posterior LV, and the interventricular septum (IVS). The tissue containing the apex is dissected into the LV and RV for sampling.
3. Cut tissue samples for DNA, GAG and SDS assays (~15 mg of wet weight).
4. Extract double-stranded DNA (dsDNA) by digesting samples in 1 M NaOH for 3 h at 65 °C and adjust pH to 7 using 10x Tris-EDTA (TE) buffer and 1 M hydrochloric acid (HCl).
5. Quantify dsDNA using a dsDNA Assay kit with a calf thymus standard (see **Table of Materials**). Read samples in duplicate using a fluorescence microplate reader (excitation at 480 nm and emission at 520 nm). Calculate the percentage of residual dsDNA in the decellularized hearts by comparing dsDNA concentration in each tissue to that in cadaveric (% cadaveric).
6. Obtain sulfated GAGs into solution by digesting tissue samples in a papain extraction solution (0.2 M sodium phosphate buffer with EDTA disodium salt, cysteine HCl, sodium acetate, and papain) at 65 °C for 3 hours. Measure GAG content (in duplicate) by using a Glycosaminoglycan Assay Kit.
7. Lyophilize samples for SDS assay in a heated vacuum and measure dry weight. Add 200 µL of ultrapure water to each dried sample and homogenize to extract the residual SDS into solution. Mix this SDS solution to chloroform and a methylene blue solution (12 mg of methylene blue in 1 L of 0.01 M HCl). The SDS will separate in the organic layer by binding to the methylene blue dye.
8. Using a fluorescence microplate reader, read the absorbance (655 nm) of the standards and samples in duplicate to calculate the residual SDS. Normalize this SDS value to tissue dry weight.
9. Image samples from thick regions (*i.e.,* LV, RV and septum) of human heart with nonlinear optical microscopy (NLOM) to confirm cellular removal after decellularization. The NLOM setup is detailed in our previous publications[18,19,20]. NLOM enables us to image cell, elastin, collagen and myosin fibers through its two-photon fluorescence (TPF) and second harmonic generation (SHG) channels without using any exogenous stain or dye[21].

Representative Results

After a 7-day decellularization with antegrade aortic perfusion under constant pressure of 120 mmHg, the human heart turned translucent (**Figure 6B**). The heart was grossly dissected into 19 sections for biochemical (DNA, GAG and SDS) analysis (**Figure 6C**) to evaluate the final decellularized product.

Throughout the decellularization process, infusion flow rate of different solutions varied as the pressure was kept constant. The flow rate into the Ao (**Figure 7A**) gradually decreased from 96.68±23.54 to 80.59±12.41 mL/min (16.64%) as the perfusion solution changed from hypertonic to hypotonic. In contrast, flow rate increased from 71.68±10.63 to 110.61±14.40 mL/min (54.31%) when perfusion solution changed from hypotonic to SDS. During the SDS perfusion, infusion flow rate fluctuated between 110±14.40 and 176.31±44.03 mL/min. The outflow rate from PA (**Figure 7B**) initially showed a similar trend (**Figure 7A**). However, the outflow rate during 1% SDS perfusion decreased from 35.77±9.07 to 27.08±4.09 mL/min. Coronary perfusion efficiency was used to evaluate aortic valve patency and similar trends. Efficiency decreased over time as different reagents perfused through the vasculature (**Figure 7C**). During the first hour of the 1X PBS wash, perfusion efficiency was restored to the original pre-hypotonic solution value (28.39±3.61% at 1-h PBS *vs.* 31.02±7.16% at 1-h hypotonic). The mean coronary perfusion efficiencies were 46.08±9.89%, 28.08±7.12%, 25.70±5.30%, and 28.39±3.61% with the hypertonic solution, the hypotonic solution, 1% SDS, and 1X PBS, respectively (**Figure 7D**).

Since the outflow perfusate from PA and LV were simultaneously collected, their debris content could be compared (**Figure 8A**) by spectroscopy absorbance measured at 280 nm (**Figure 8B**). The turbidity of the effluent from PA and LV decreased over time during perfusion of each solution; however, turbidity from the PA showed a more abrupt color change as compared to that observed from LV during the initial perfusion period. After switching from a hypertonic to a hypotonic solution, the turbidity of PA outflow changed from 1.15±0.03 to 1.40±0.07 (21.73% increase) and of LV changed from 1.13±0.05 to 1.24±0.07 (9.73% increase). During the first hour of 1% SDS perfusion, turbidity changed from 1.17±0.04 to 2.77±0.15 (136.75% increase) for PA and 1.11±0.04 to 1.75±0.26 (56.65% increase) for the LV effluent. The correlation between outflow turbidity and cell debris washout was evaluated using the bicinchoninic acid (BCA) protein assay when protein concentration was quantified in the outflow samples. The results obtained from the decellularization of 6 human hearts revealed a linear correlation between protein concentration and effluent turbidity with $R^2 = 0.95$ (**Figure 8C**).

After completion of whole-heart decellularization, the coronary angiogram confirmed the preservation of intact coronary vasculature (**Figure 9**). Nonlinear optical imaging of myocardium layers from thick areas (*i.e.,* RV, LV, and septum) in decellularized human heart confirmed cell removal, as no cell presence was observed in TPF channels (**Figure 10**). Cells (*i.e.,* cardiomyocytes or cardiac fibroblasts) with their autofluorescence can be easily identified in TPF channel by their oval and elongated shape morphologies. To ensure effectiveness of the decellularization process and cellular debris removal, the decellularized human hearts were further grossed into 19 regions (**Figure 6C**) to quantify the levels of DNA, sulfated GAGs, and SDS remaining in those regions. DNA in all regions was less than 10% of cadaveric heart. DNA in right atrium (8.39%-10.38% relative to cadaveric) and left atrium (5.11%-7.60%) was highest (**Figure 11A**).

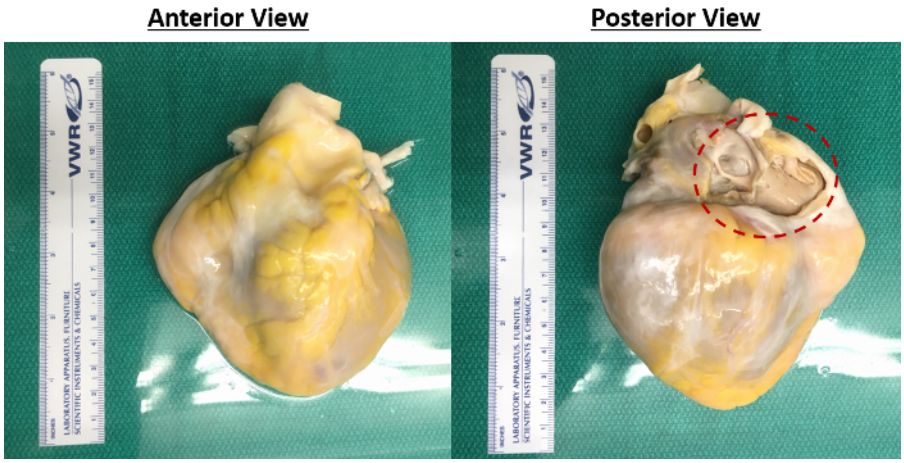

Figure 1: Cadaveric human heart from an organ procurement agency. Anterior and posterior views of cadaveric human heart. Inferior vena cava and a portion of right atrium are missing, as observed in dashed region. Please click here to view a larger version of this figure.

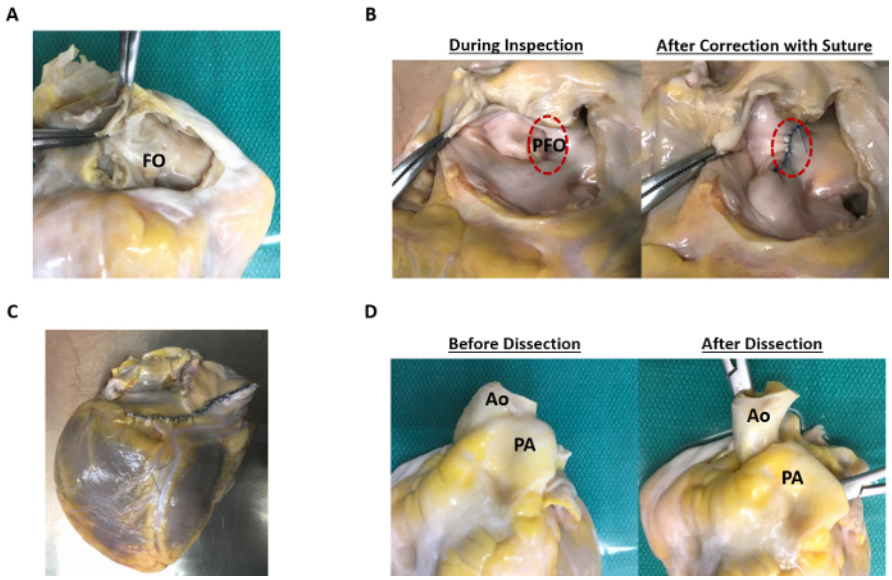

Figure 2: Inspection for septal and/or valve anatomical anomalies. (A) Inspect if patent foramen ovale (PFO) is present (communication between right and left atrium). **(B)** A 5-0 polypropylene suture is applied in a continuous fashion to close PFO. **(C)** Right atrium is closed with a running suture of 5-0 polypropylene. **(D)** The main pulmonary artery is dissected away from the ascending aorta by blunt dissection. FO: foramen ovale; PA: pulmonary artery; Ao: aorta. Please click here to view a larger version of this figure.

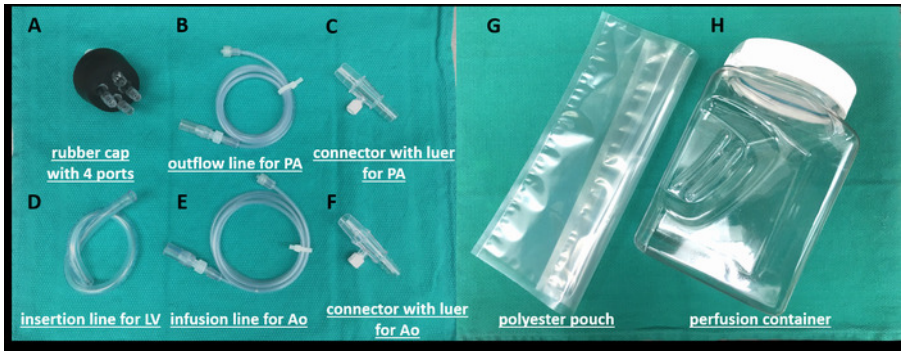

Figure 3: Components of the infusion bioreactor. The decellularization system is composed of **(A)** rubber cap with 4 ports; **(B)** outflow line to be connected to the pulmonary artery (PA); **(C, F)** connectors with luer lock for PA and aorta (Ao), **(D)** insertion line for the left ventricle (LV), **(E)** infusion line to be connected to the aorta, **(G)** polyester pouch, and **(H)** Perfusion container. Please click here to view a larger version of this figure.

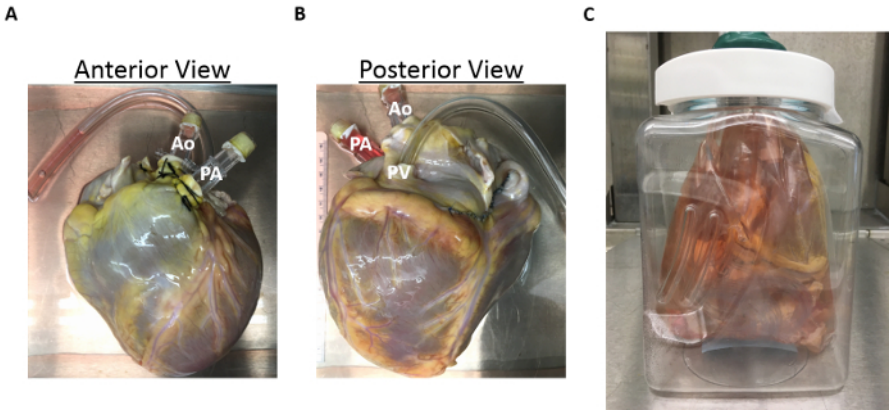

Figure 4: Human heart cannulation and infusion bioreactor assembly. (A) Anterior view of the heart showing pulmonary artery (PA) and aorta (Ao) individually cannulated. **(B)** Posterior view of the heart showing cannula directed to left ventricle (LV) through pulmonary vein (PV). **(C)** Human heart inside the Infusion bioreactor after assembly. Please click here to view a larger version of this figure.

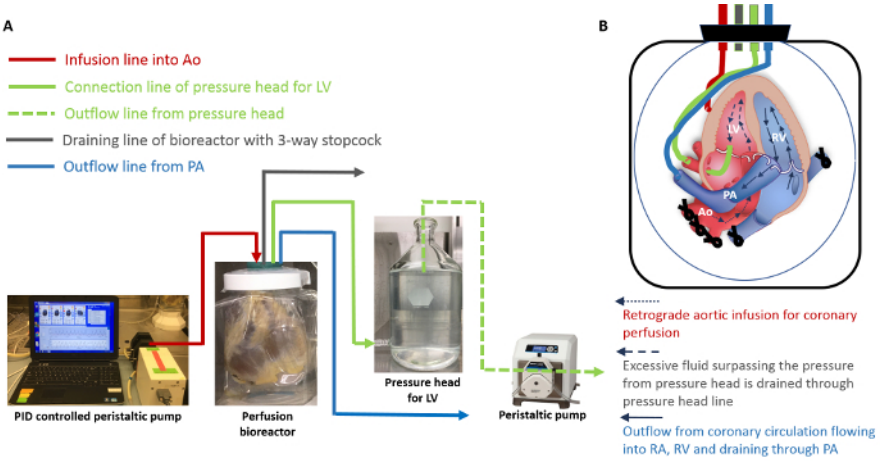

Figure 5: System setup of inverted oriented decellularization with pressure head. (A) The complete decellularization system is composed of: a computer, a proportional-integral-derivative (PID) controller, pumps, a bioreactor, and reservoirs for collecting the effluent from pulmonary artery (PA) and left ventricle (LV). Ao: aorta. Arrows indicate flow direction. **(B)** The schematic of the setup of human heart inside perfusion bioreactor and the associated flow paths of perfusate/effluent during decellularization. Please click here to view a larger version of this figure.

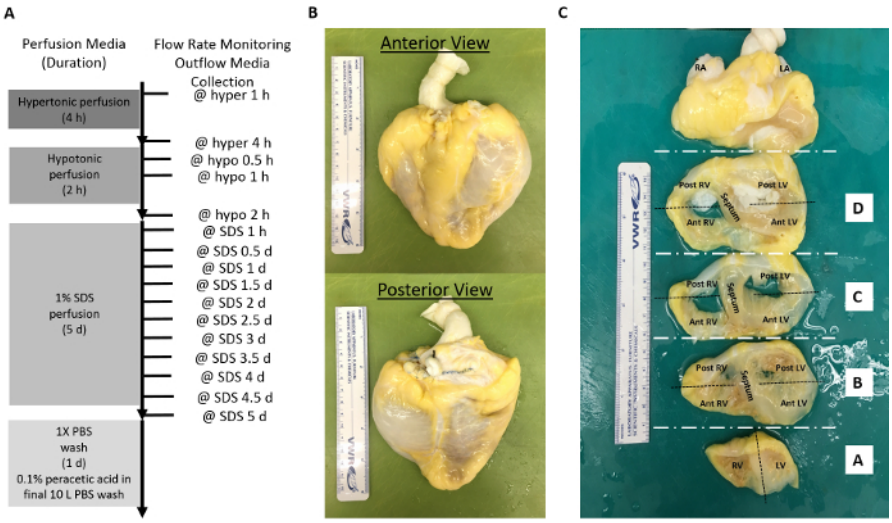

Figure 6: Schematic representation of the decellularization procedure and post-decellularization examination of a human heart. (A) Diagram of the decellularization procedure. **(B)** Anterior and posterior examination of a decellularized human heart. **(C)** Gross dissection of a human heart into four cross-sections (section A to section D) for biochemical assay analysis. The coloring in the human hearts is caused by residual lipofucin deposition. The coloring normally presents in inner ventricular surface or the boundary between epicardium and myocardium. LA: left atrium; RA: right atrium; LV: left ventricle; RV: right ventricle; Ant: anterior; Post: posterior; Hyper: hypertonic; Hypo: hypotonic; SDS: sodium dodecyl sulfate; PBS: phosphate buffered saline. Please click here to view a larger version of this figure.

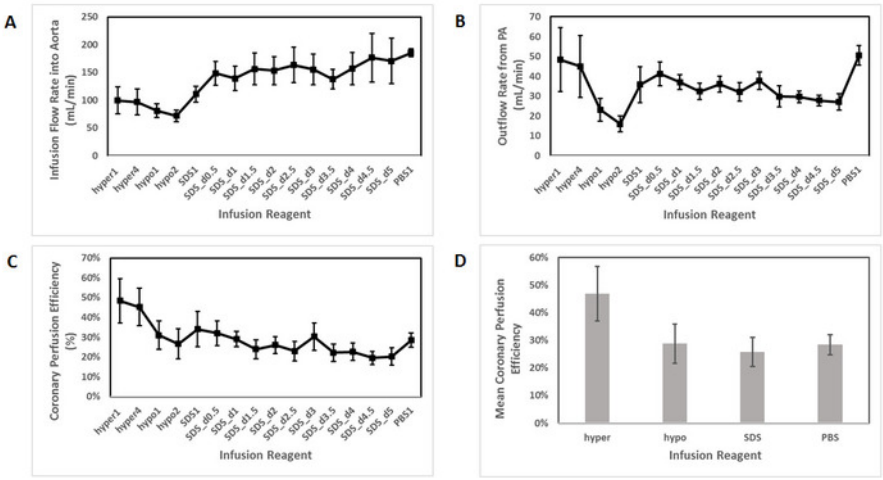

Figure 7: Time-lapse flow dynamics during decellularization. (A) Infusion flow rate of decellularization solutions into aorta during procedure. **(B)** Flow rate of effluent from PA during decellularization. **(C)** Coronary perfusion efficiency during decellularization. **(D)** Mean coronary perfusion efficiency during perfusion of different solutions/reagents. N = 6. Data represent mean±SEM. PA: pulmonary artery; Hyper: hypertonic; Hypo: hypotonic; SDS: sodium dodecyl sulfate; PBS: phosphate buffered saline; SEM: standard error of mean. Please click here to view a larger version of this figure.

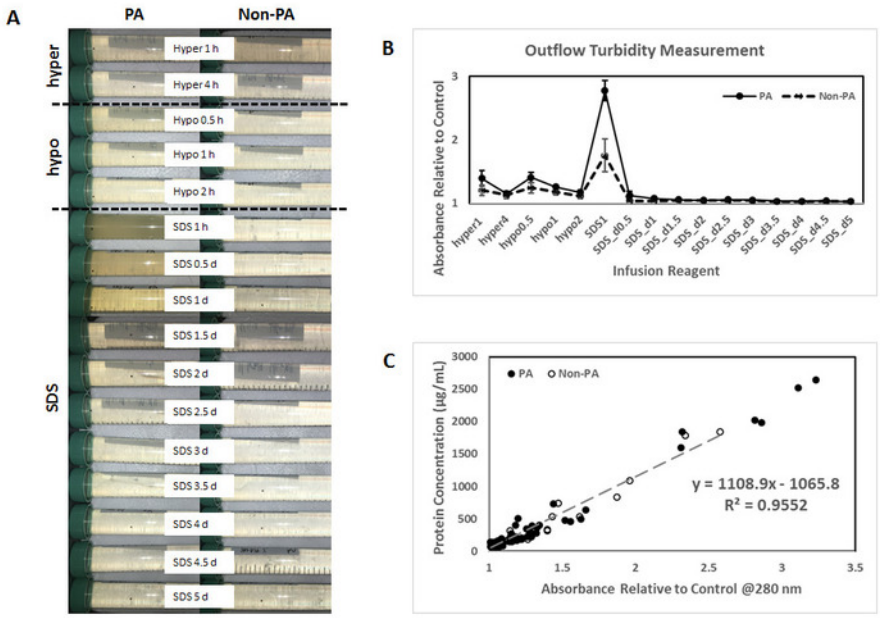

Figure 8: Time-lapse cell debris washout during decellularization. (A) Outflow media collection from PA and non-PA (Left ventricle). **(B)** Result of turbidity measurement at 280 nm. **(C)** Linear correlation exists between protein concentration and turbidity. n = 6 human hearts. Control was clean decellularization solution. Data represent mean±SEM. PA: pulmonary artery; Hyper: hypertonic; Hypo: hypotonic; SDS: sodium dodecyl sulfate; SEM: standard error of mean. Please click here to view a larger version of this figure.

Figure 9: Coronary angiogram of decellularized human heart confirms thevascular patency after decellularization. Please click here to view a larger version of this figure.

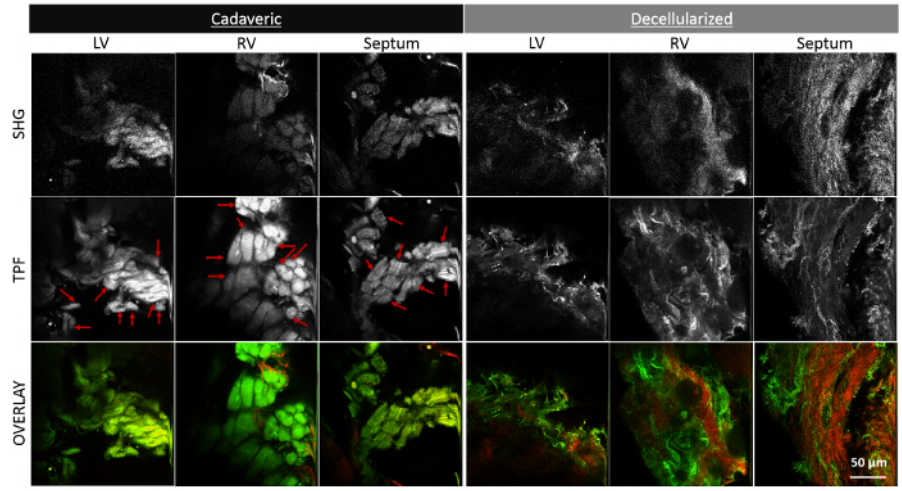

Figure 10: Images obtained using nonlinear optical microscopy from cadaveric and decellularized myocardium show no presense of cells (*i.e.,* cardiomyocytes or cardiac fibroblasts) with oval or elongated shape morphologies in the decellularized LV, RV and septum. LV: left ventricle; RV: right ventricle; TPF: two photon fluorescence; SHG: second harmonic generation. Some cardiac cells are indicated by arrows. Please click here to view a larger version of this figure.

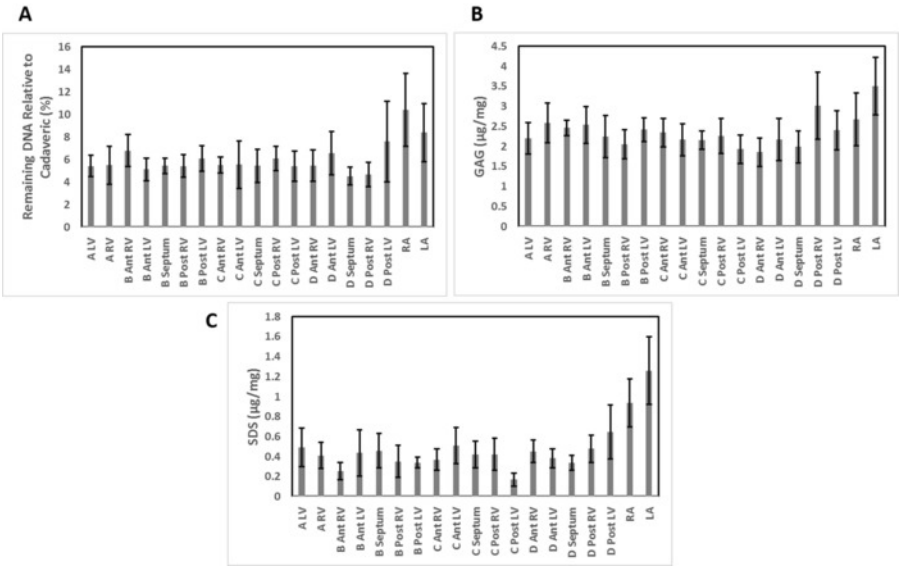

Figure 11: Biochemical assay results. (A) Remaining DNA relative to cadaveric heart in decellularized tissues. **(B)** Remaining GAG relative to cadaveric heart in decellularized tissues. **(C)** Remaining SDS in decellularized tissues. n = 6 human hearts. Data represent mean±SEM. LA: left atrium; RA: right atrium; LV: left ventricle; RV: right ventricle; Ant: anterior; Post: posterior; SDS: sodium dodecyl sulfate; SEM: standard error of mean. Please click here to view a larger version of this figure.

Method	*Pro*	*Con*
Conventional upright Langendorff perfusion	· Easy to access the heart to repair during decellularization	· Excessive strain on the aorta owing to heart weight
		· High infusion flow rate during SDS perfusion under constant pressure control
		· Low coronary perfusion efficiency during SDS perfusion
		· The portion of aorta/pulmonary artery above cannula ligation line could get dehydrated and easily contaminated
Inverted Langendorff perfusion inside a pressurized pouch	· Minimize strain exerted on the aorta owing to heart weight	· Hard to access the heart if repairing is needed.
	· Low infusion flow rate during SDS perfusion under constant pressure control	
	· Improved coronary perfusion efficiency during SDS perfusion	
	· No tissues will be dried out since the whole heart is submerged/hydrated.	

Table 1: A summary of pros and cons of whole-heart decellularization using conventional upright perfusion vs. inverted Langendorff perfusion inside a pressurized pouch.

Discussion

To our knowledge, this is the first study to report inverted decellularization of human hearts inside a pressurized pouch with time-lapse monitoring of flow rate and cell debris removal. The pericardium-like pouch keeps the orientation of the heart stable throughout the decellularization procedure. Submerging and inverting the whole hearts inside a pouch prevents dehydration and minimizes excessive strain on the aorta (from heart weight) when compared to the conventional upright Langendorff perfusion decellularization method[9]. This, in turn, preserves the competency of the aortic valve.

To achieve maximal decellularization efficiency, coronary vascular resistance must be low to ensure adequate and consistent perfusion of fluid through the entire myocardium. In the whole-heart decellularization model using retrograde perfusion, fluid accumulates in the ventricles and elevates intraventricular pressure, which, in turn, increases coronary vascular resistance and limits the flow of fluids. Even though the aortic valve is intact, the ventricular cavity fills secondary to physiological leakage and in turn compresses the ventricular wall.

Our technique of decellularizing a heart inside a pressurized pouch is aimed to alleviate this problem and increase decellularization efficiency. A pressure of 120 mmHg at the aortic root and 14 mmHg in the pouch is maintained throughout the decellularization process. These pressure values are very close to physiological range (80-120 mmHg in aorta and 15 mmHg for Left ventricular end-diastolic pressure[22]). According to Murthy *et al.*[23], the myocardial blood flow rate ranges from 0.61 to 1.10 mL/min/g, and the human heart weight[24,25] is about 245 to 308 g; hence, the physiological coronary flow rate is about 149.45 to 338.80 mL/min, but depends on heart weight. Our outflow rate from PA ranged from 20 to 50 mL/min, which is less than the value of physiological coronary flow rate and could have resulted from 2 different situations: 1) the infusion of solutions to the heart produce edema and there is also normal anatomical drainage of the coronary system to the left ventricle cavity; 2) as the decellularization occurs, liquid is also lost through the decellularized walls due to a natural increase in their permeability. This pressure differential prevents collapse of the vessels and allows them to remain patent. Moreover, this system maintains the heart in relative anatomic conditions without compressing the myocardial wall, which would increase coronary vascular resistance and impair the intravascular circulation of the decellularization solutions. The infusion flow rate profile of human hearts (**Figure 7A**) is very similar to what we observed in our inverted decellularization of porcine heart[9], with lowest infusion flow rate occurring during the hypotonic perfusion and a slight increase in flow rate (110.61±14.40 mL/min to 176.31±44.03 mL/min) occurring during 1% SDS perfusion. Our infusion flow rate (mean value=151.50±3.71 mL/min) during 1% SDS perfusion was comparable to, or even less than that for human heart decellularization reported by Guyette *et al.*[14] However, our method is performed with pressure control of 120 mmHg and their method used 60 mmHg. This difference in perfusion pressures suggests a superior effectiveness of aortic valve closure in our technique since a lower infusion flow rate could maintain higher pressure. Another possibility is that the increased coronary resistance was due to the applied 14 mmHg pressure inside the pouch. Additionally, our human heart method showed a similar trend of decreasing coronary perfusion efficiency (~30%, **Figure 7C**, **7D**) from hyper to hypotonic solution change when compared to our inverted porcine heart decellularization (~10% in inverted orientation[9] *vs.* 1-2% in upright orientation). However, this novel method could preserve coronary perfusion efficiency during SDS perfusion comparable to solution perfusion and thus appears superior to our prior method of sample inversion. **Table 1** lists the pros and cons of conventional upright perfusion *vs.* inverted Langendorff perfusion inside a pressurized pouch.

In addition to flow rate, outflow turbidity monitoring could be another useful tool to evaluate decellularization progress and efficiency. During decellularization, turbidity of the effluent from the PA was higher than that of the effluent from non-PA sites (**Figure 8B**). This suggests that most of the perfused solution was going through the vasculature for "proper" decellularization. Yet for this to be valid, the following must be addressed: inter-chamber shunts, or patency of the aortic valve. Careful and meticulous inspection is therefore needed to prevent failure of the method due to anatomical non-conformities. The turbidity profile (**Figure 8B**) of the whole heart decellularization process demonstrated similar trends as previously shown, with abrupt turbidity change during the initial transition period of different perfusates[9].

A main goal for decellularized tissues is to be able to repopulate them with cells and achieve high cell attachment, proliferation, maturation and functionality. Our decellularized tissues have been successfully cellularized for various applications[26,27], where the tissues were successfully cellularized and achieved lower thrombogenicity. In our biochemical analyses of decellularized human hearts, we evaluated 19 regions with different tissue thicknesses. The DNA and SDS in decellularized tissues varied, with the highest value obtained in the right and left atrium. This could be caused by the orientation of the heart in an upside-down configuration, wherein cell debris was trapped at the bottom of the pouch or where external pressure reduced flow. Perfusion decellularization relies on undamaged heart structures, including intact coronaries and tributaries. As these organs are procured from multi-organ donors, these hearts usually have a large portion of their atria removed. During the preparation of these organs and repair of the atrial wall, there was disruption in the irrigation of these regions, jeopardizing the flow of the decellularization solutions. For non-perfusion heart decellularization, other research groups have reported 2-6% leftover DNA in rat[28], porcine[29,30] and human[31] as compared with respective cadaveric heart. However, they used freeze-thaw[28,29,30], enzyme[29,30] and serum[31] in their decellularization protocol, which may damage the ECM to a greater degree than our perfusion-based technique. Developing methods to adequately address these limitations will be critical.

Disclosures

Dr. Taylor is the founder and shareholder in Miromatrix Medical, Inc. This relationship is managed in accordance with the conflict of interest policies by the University of Minnesota and Texas Heart Institute; the other authors have no conflict of interest to disclose.

Acknowledgements

This research was supported by the Houston Endowment grant and the Texas Emerging Technology Fund. The authors acknowledge the organ procurement agency LifeGift, Inc. and the donor's families for making this study possible.

References

1. Writing Group Members, *et al.* Executive Summary: Heart Disease and Stroke Statistics--2016 Update: A Report From the American Heart Association. *Circulation.* **133** (4), 447-454, (2016).
2. Zia, S. *et al.* Hearts beating through decellularized scaffolds: whole-organ engineering for cardiac regeneration and transplantation. *Critical Reviews in Biotechnology.* **36** (4), 705-715, (2016).
3. Zimmermann, W. H. Strip and Dress the Human Heart. *Circulation Research.* **118** (1), 12-13, (2016).
4. Ott, H. C. *et al.* Perfusion-decellularized matrix: Using nature's platform to engineer a bioartificial heart. *Nature Medicine.* **14** (2), 213-221, (2008).
5. Sanchez, P. L. *et al.* Acellular human heart matrix: A critical step toward whole heart grafts. *Biomaterials.* **61**, 279-289, (2015).
6. Peloso, A. *et al.* Current achievements and future perspectives in whole-organ bioengineering. *Stem Cell Research & Therapy.* **6**, 107, (2015).
7. Guyette, J. P. *et al.* Perfusion decellularization of whole organs. *Nature Protocols.* **9** (6), 1451-1468, (2014).
8. Momtahan, N., Sukavaneshvar, S., Roeder, B. L., & Cook, A. D. Strategies and Processes to Decellularize and Cellularize Hearts to Generate Functional Organs and Reduce the Risk of Thrombosis. *Tissue Engineering Part B-Reviews.* **21** (1), 115-132, (2015).
9. Lee, P. F. *et al.* Inverted orientation improves decellularization of whole porcine hearts. *Acta Biomaterialia.* (2016).
10. Momtahan, N. *et al.* Automation of Pressure Control Improves Whole Porcine Heart Decellularization. *Tissue Eng Part C Methods.* (2015).
11. Weymann, A. *et al.* Development and Evaluation of a Perfusion Decellularization Porcine Heart Model - Generation of 3-Dimensional Myocardial Neoscaffolds. *Circulation Journal.* **75** (4), 852-860, (2011).
12. Weymann, A. *et al.* Bioartificial heart: A human-sized porcine model--the way ahead. *PLoS One.* **9** (11), e111591, (2014).
13. Remlinger, N. T., Wearden, P. D., & Gilbert, T. W. Procedure for decellularization of porcine heart by retrograde coronary perfusion. *Journal of Visualized Experiments.* (70), e50059, (2012).
14. Guyette, J. P. *et al.* Bioengineering Human Myocardium on Native Extracellular Matrix. *Circulation Research.* **118** (1), 56-72, (2016).
15. Sanchez, P. L. *et al.* Data from acellular human heart matrix. *Data Brief.* **8**, 211-219, (2016).
16. Garreta, E. *et al.* Myocardial commitment from human pluripotent stem cells: Rapid production of human heart grafts. *Biomaterials.* **98**, 64-78, (2016).
17. Wainwright, J. M. *et al.* Preparation of Cardiac Extracellular Matrix from an Intact Porcine Heart. *Tissue Engineering Part C-Methods.* **16** (3), 525-532, (2010).
18. Larson, A. M., & Yeh, A. T. *Ex vivo* characterization of sub-10-fs pulses. *Optics Letters.* **31** (11), 1681-1683, (2006).
19. Lee, P. F., Yeh, A. T., & Bayless, K. J. Nonlinear optical microscopy reveals invading endothelial cells anisotropically alter three-dimensional collagen matrices. *Experimental Cell Research.* **315** (3), 396-410, (2009).
20. Lee, P. F., Bai, Y., Smith, R. L., Bayless, K. J., & Yeh, A. T. Angiogenic responses are enhanced in mechanically and microscopically characterized, microbial transglutaminase crosslinked collagen matrices with increased stiffness. *Acta Biomaterialia.* **9** (7), 7178-7190, (2013).
21. Wu, Z. *et al.* Multi-photon microscopy in cardiovascular research. *Methods.* **130**, 79-89, (2017).
22. Ramanathan, T., Skinner, H. Coronary blood flow. *Continuing Education in Anaesthesia Critical Care & Pain.* **5** (2), 61-64, (2005).
23. Murthy, V. L. *et al.* Clinical Quantification of Myocardial Blood Flow Using PET: Joint Position Paper of the SNMMI Cardiovascular Council and the ASNC. *Journal of Nuclear Cardiology.* **25** (1), 269-297, (2018).
24. Molina, D. K., & DiMaio, V. J. Normal organ weights in men: Part I-the heart. *The American Journal of Forensic Medicine and Pathology.* **33** (4), 362-367, (2012).
25. Molina, D. K., & DiMaio, V. J. Normal Organ Weights in Women: Part I-The Heart. *The American Journal of Forensic Medicine and Pathology.* **36** (3), 176-181, (2015).
26. Robertson, M. J., Dries-Devlin, J. L., Kren, S. M., Burchfield, J. S., & Taylor, D. A. Optimizing cellularization of whole decellularized heart extracellular matrix. *PLoS One.* **9** (2), e90406, (2014).

27. Robertson, M. J., Soibam, B., O'Leary, J. G., Sampaio, L. C., & Taylor, D. A. Cellularization of rat liver: An *in vitro* model for assessing human drug metabolism and liver biology. *PLoS One*. **13** (1), e0191892, (2018).
28. Baghalishahi, M. *et al.* Cardiac extracellular matrix hydrogel together with or without inducer cocktail improves human adipose tissue-derived stem cells differentiation into cardiomyocyte-like cells. *Biochemical and Biophysical Research Communications.* (2018).
29. Perea-Gil, I. *et al*. *In vitro* comparative study of two decellularization protocols in search of an optimal myocardial scaffold for cellularization. *American Journal of Translational Research.* **7** (3), 558-573, (2015).
30. Freytes, D. O., O'Neill, J. D., Duan-Arnold, Y., Wrona, E. A., & Vunjak-Novakovic, G. Natural cardiac extracellular matrix hydrogels for cultivation of human stem cell-derived cardiomyocytes. *Methods Molecular Biology.* **1181**, 69-81, (2014).
31. Oberwallner, B. *et al.* Preparation of cardiac extracellular matrix scaffolds by decellularization of human myocardium. *Journal of Biomedical Materials Research Part A.* **102** (9), 3263-3272, (2014).

